HHS Public Access

Author manuscript

J Leukoc Biol. Author manuscript; available in PMC 2022 February 17.

Published in final edited form as:

J Leukoc Biol. 2021 April ; 109(4): 793–806. doi:10.1002/JLB.3A0320-210R.

Neutrophils produce proinflammatory or anti-inflammatory extracellular vesicles depending on the environmental conditions

Ferenc Kolonics[1], **Erika Kajdácsi**[2], **Veronika J. Farkas**[3], **Dániel S. Veres**[4], **Delaram Khamari**[5], **Ágnes Kittel**[6], **Michael L. Merchant**[7], **Kenneth R. McLeish**[7], **Ákos M. Lőrincz**[1], **Erzsébet Ligeti**[1]

[1]Department of Physiology, Semmelweis University, Budapest, Hungary

[2]Research Laboratory of the 3rd Department of Internal Medicine, Semmelweis University, Budapest, Hungary

[3]Department of Medical Biochemistry, Semmelweis University, Budapest, Hungary

[4]Department of Biophysics and Radiation Biology, Semmelweis University, Budapest, Hungary

[5]Department of Genetics and Immunobiology, Semmelweis University, Budapest, Hungary

[6]Institute of Experimental Medicine, Eötvös Loránd Research Network (ELRN), Budapest, Hungary

[7]Department of Medicine, University of Louisville, Louisville, Kentucky, USA

Abstract

Extracellular vesicles (EVs) are important elements of intercellular communication. A plethora of different, occasionally even opposite, physiologic and pathologic effects have been attributed to these vesicles in the last decade. A direct comparison of individual observations is however hampered by the significant differences in the way of elicitation, collection, handling, and storage of the investigated vesicles. In the current work, we carried out a careful comparative study on 3, previously characterized types of EVs produced by neutrophilic granulocytes. We investigated in parallel the modulation of multiple blood-related cells and functions by medium-sized vesicles. We show that EVs released from resting neutrophils exert anti-inflammatory action

Correspondence Erzsébet Ligeti, Department of Physiology, Semmelweis University, H-1095, Budapest, Tűzoltó u. 37-47, Hungary. ligeti.erzsebet@med.semmelweis-univ.hu.

AUTHORSHIP

F.K. carried out most of the experiments, prepared the figures, and participated in writing of the manuscript. E.K. and V.J.F. provided expertise and were involved in experiments on HUVEC and coagulation, respectively. D.S.V. carried out the DLS measurements. D.K. carried out the NTA measurements. M.L.M. and K.R.M. did the proteomic analysis. Á.M.L. analyzed the proteomic data. Á.M.L. and E.L. designed and supervised the study and wrote most part of the manuscript. E.L. obtained financing. Á.M.L. and E.L. contributed equally to this work.

DISCLOSURES

The authors declare no conflicts of interest.

SUPPORTING INFORMATION

Additional information may be found online in the Supporting Information section at the end of the article.

by reducing production of reactive oxygen species (ROS) and cytokine release from neutrophils. In contrast, vesicles generated upon encounter of neutrophils with opsonized particles rather promote proinflammatory processes as they increase production of ROS and cytokine secretion from neutrophils and activate endothelial cells. EVs released from apoptosing cells were mainly active in promoting coagulation. We thus propose that EVs are “custom made,” acquiring selective capacities depending on environmental factors prevailing at the time of their biogenesis.

Keywords

reactive oxygen species; IL-8 secretion; phagocytosis; migration; coagulation; endothelial cells

1 | INTRODUCTION

Generation of extracellular vesicles (EV) is a common property of cells. Intensive research of the last decade has revealed a multitude of different biologic—both physiologic and pathologic—effects of EVs.[1,2] Following a significant number of preclinical studies,[3,4] initial attempts of therapeutic applications using EVs or EV-related drug delivery have started.[5,6] However, comparative data on specificity and selectivity of the effect of defined EV populations are still scarce.[7-10]

Neutrophilic granulocytes (PMNs) represent the most abundant population of leukocytes in circulating blood. As they are active in formation of EVs, PMN-derived EVs constitute a large fraction of EVs in normal blood. The number of PMN-derived EVs was reported to become significantly elevated in various pathologic conditions.[2,11,12] The effects of neutrophil-derived EVs have been extensively investigated on almost every blood-related cell type and function, including neutrophils themselves,[13-16] monocytes,[17] monocyte-derived macrophages[17-25] and dendritic cells,[26] lymphocytes,[27] endothelial cells,[28,29] and coagulation.[30]

Most studies demonstrated dominant anti-inflammatory effect of PMN-EVs on the interacting cells, by decreasing the production of activating cytokines such as IL-1β, TNFα, IL-6, IL-8, IL-10, or IL-12[17-21,26] and increasing the secretion of TGFβ or resolving mediators.[17,20,25,26] Opposing effects have also been reported, such as an increase in IL-6 and IL-8 production from, and expression of adhesion molecules on, endothelial cells[29]; enhanced superoxide, IL-6 and TNFα secretion from macrophages,[13,18] and stimulation of LTB4 synthesis in neutrophils.[15] Enhanced coagulation has also been reported.[30] These studies typically investigated the effects of PMN-EVs on 1 single cell type or function. A wide variety of EVs were applied, including true exosomes[15] and microvesicles/ectosomes produced spontaneously or upon various stimuli.[13,17-21,25,26,29,30] However, the differences between the effects of differently produced EVs were only rarely analyzed.[18,31] Lastly, in many investigations, EVs were stored frozen for undefined periods.

In previous work, our group has characterized 3 different types of PMN-EVs in detail: those produced spontaneously in short incubation from resting cells (sEV), those produced by apoptotic cells in 1–3 days (apoEV), and those generated upon stimulation with opsonized particles.[12,32] Only the latter EV population was able to impair bacterial growth in a

concentration-dependent manner[12,33]; hence, they were named “antibacterial EVs” (aEV). However, antibacterial capacity was lost under different storage conditions in a relatively short time.[34] In several tests, sEV and apoEV were more similar to each other than either of them to aEV.[32] Hence, the question arises whether sEV, apoEV, and aEV only differ in their antibacterial capacity or also in their effects on other blood cells and functions.

The aim of the present study was to compare the effects of 3, previously well-characterized PMN-EV types, applied freshly after isolation, on cells and function they could affect in their natural environment by autocrine or paracrine mechanisms, such as neutrophils themselves, endothelial cells, and coagulation of pooled human plasma. We demonstrate selective effects in all of the investigated functions.

2 | METHODS

2.1 | Materials

HBSS with calcium, magnesium, and glucose was from GE Healthcare Life Sciences (South Logan, UT, USA); zymosan A was from Sigma–Aldrich (St. Louis, MO, USA); Ficoll-Paque from GE Healthcare BioSciences AB (Uppsala, Sweden); HEPES (pH 7.4) from Sigma. All other used reagents were of research grade.

GFP expressing and chloramphenicol-resistant *Staphylococcus aureus (USA300)* was a kind gift from Professor William Nauseef (University of Iowa).

2.2 | Isolation of human PMNs and monocytes

Venous blood samples were drawn from healthy adult volunteers according to the procedures approved by the National Ethical Committee (ETT-TUKEB No. BPR/021/01563-2/2015). The age and gender distribution of our donors was the following: 32.5% of the donors were women, 67.5% were men. Mean age was 24.8±6.5 years; the youngest donor was 19, the oldest was 55 years old.

Neutrophils were obtained by dextran sedimentation followed by a 62.5% (v/v) Ficoll gradient centrifugation (Beckman Coulter Allegra X-15R, 1,000 *g*, 20 min, 22°C) as previously described.[35] The mononuclear cell layer (consisting of lymphocytes and monocytes) was extracted by pipetting after the Ficoll gradient centrifugation step. Contaminating red blood cells were removed by hypotonic lysis. Cells were finally resuspended in HBSS and kept on ice until use. The neutrophil preparations contained more than 95% PMNs and less than 0.5% eosinophils.

2.3 | Opsonization

Zymosan A (5 mg in 1 ml HBSS) was opsonized with 500 µl prewarmed pooled human serum for 25 min at 37°C. After opsonization, zymosan was centrifuged (5,000 *g*, 5 min, 4°C, Hermle Z216MK 45° fixed angle rotor), and washed once in HBSS.

USA300 bacteria (OD_{600} = 1.0 in 900 µl HBSS) were opsonized with 100 µl prewarmed pooled human serum for 25 min at 37°C. After opsonization, bacteria were centrifuged (5,000 *g*, 5 min, 4°C), and washed once in HBSS.

2.4 | Preparation of EV fractions

PMNs(10^7 cells in 1 ml HBSS) were left unstimulated or were activated by 0.5 mg/ml final concentration of opsonized zymosan A for 20 min at 37°C in a linear shaker (0.18 g). Spontaneous cell death was initiated in HBSS by leaving PMNs (2.5×10^6 cells/ml HBSS) unstimulated at 37°C for 24 h. After incubation, cells were sedimented (Hermle Z216MK 45° fixed angle rotor, 500 *g*, 5 min, 4°C). The supernatant was filtered through a 5 μm pore sterile filter (Sterile Millex Filter Unit, Millipore, Billerica, MA, USA). The filtered fraction was sedimented (15,700 g, 10 min, 4°C) and the sediment was resuspended in HBSS at the original incubation volume unless indicated otherwise. By this procedure, we got 3 different EV types as characterized previously[32]: activated EVs (aEVs) from opsonized zymosan A activated cells in 20 min, spontaneously generated EVs (sEVs) from unstimulated cells in 20 min, and apoptotic EVs (apoEVs) from cells undergoing spontaneous cell death. Apoptotic EVs originated from the PMN preparation of the preceding day of the indicated experiment.

As zymosan residues arising from the cell activation are an inherent, inseparable part of aEV fractions after the EV isolation process, we prepared a control sample for aEV measurements, which contained the same amount of zymosan as aEV isolates. To achieve this, half of the aEV batch was sedimented (15,700 g, 10 min, 4°C), resuspended in distilled water at the original volume, vortexed for 10 min, then sedimented again (15,700 g, 10 min, 4°C), and resuspended in HBSS at the same volume as the aEV sample. By this means, relevant EV fractions were destroyed due to hypotonic lysis and mechanical disruption, zymosan particles however are resistant to both. We refer to this sample as “lysed aEV.”

2.5 | Characterization of the size distribution of PMN-derived EVs

Dynamic light scattering (DLS) measurements were performed at room temperature with an equipment consisting of a goniometer system (ALV GmbH, Langen, Germany), a diode-pumped solid-state laser light source (Melles Griot, IDEX corp., Lake Forest, IL, USA; 58-BLS-301, 457 nm, 150 mW), and a light detector (Hamamatsu, Japan; H7155 PMT module). The evaluation software yielded the autocorrelation function of scattered light intensity, which was further analyzed by the maximum entropy method, from where the different contributions of this function were determined. The radius of the particles was calculated using sphere approximation.[36]

For nanoparticle tracking analysis (NTA), samples were resuspended in 1 ml of PBS to reach appropriate particle concentration range for the measurement. Particle size distribution and concentration were analyzed on ZetaView PMX120 instrument (Particle Metrix, Inning am Ammersee, Germany). For each measurement, 11 cell positions were scanned at 25°C (in 2 cycles) with the following camera settings: shutter speed—100, sensitivity—75, frame rate—7.5, video quality—medium (30 frames). The videos were analyzed by the ZetaView Analyze software 8.05.10 with a minimum area of 5, maximum area of 1,000, and a minimum brightness of 20.

2.6 | Transmission electron microscopic investigation of the PMN-derived EVs

EV-containing pellets were processed as described in our previous papers.[12,36] Briefly, pelleted EVs were fixed with 4% paraformaldehyde at room temperature for 1 h, rinsed

by PBS, and post-fixed in 1% osmium tetroxide (OsO_4) for 20 min. After rinsing with distilled water, pellets were dehydrated by a series of increasing ethanol concentrations, including block staining with 1% uranyl-acetate in 50% ethanol for 30 min, finally embedded in Taab 812 (Taab, Aldermaston, UK). Following polymerization at 60°C for 12 h, 50–60 nm ultrathin sections were cut using a Leica UCT ultramicrotome (Leica Microsystems, Wetzlar, Germany, UK) and examined using a Hitachi 7100 transmission electron microscope (TEM) (Hitachi Ltd.,Tokio, Japan).

Electron micrographs were made by Veleta 2k x 2k Megapixel side-mounted TEM CCD camera (Olympus, Tokio, Japan). Contrast/brightness of electron micrographs was edited by Adobe Photoshop CS4 (Adobe Systems Incorporated, San Jose, CA, USA).

2.7 | Antibacterial activity of different types of PMN-derived EVs

Opsonized bacteria (5×10^7/50 µl HBSS) were added to 500 µl EV (derived from 5×10^6 PMNs) suspended in HBSS. During a 40 min coincubation step at 37°C, the bacterial count decreases or increases depending on the samples' antibacterial effect and the growth of bacteria. At the end of the incubation, 2 ml ice-cold stopping solution (1 mg/ml saponin in HBSS) was added to stop the incubation and lyse EVs. After a freezing step at −80°C for 20 min, samples were thawed to room temperature and inoculated into LB broth. Bacterial growth was followed as changes in OD using a shaking microplate reader (Labsystems iEMS Reader MF; Thermo Scientific, Waltham, MA, USA) for 8 h, at 37°C, at 650 nm. After the end of growth phase, the initial bacterial counts were calculated indirectly using an equation similar to PCR calculation, as described previously.[35]

2.8 | Investigation of the EV uptake by leukocytes

All aEVs, sEVs, and apoEVs were stained with PKH67 (Sigma) in 4 µM final concentration for 5 min. To wash out unbound PKH67, after sedimentation of the EVs (15,700 g, 10 min, 4°C), the pellet was resuspended in HBSS at double of the original volume. After 10 min incubation at room temperature, EVs were sedimented again (15,700 g, 10 min, 4°C) and resuspended at the original volume. One part of the EVs was pelleted for a 3rd time (15,700 g, 10 min, 4°C) and the supernatant was used as control for unspecific PKH binding.

PMN (50 µL of 5×10^6/ml) or mononuclear cell suspension (50 µl of 10^7/ml) was added to 500 µl aEV, sEV, apoEV sample or to the control supernatant. EVs and cells were coincubated for 45 min in a linear shaker (0.18 g) at 37°C. aEV and sEV samples were prepared from 10^7 cells, whereas apoEV samples were derived from 1.25×10^6 cells.

For flow cytometric (FC) detection of EV uptake, a Becton Dickinson FACSCalibur flow cytometer was used with the following settings: flow rate was held under 1,000 events/s; forward scatter (FSC) = E–1 (log); side scatter (SSC) = 320 V (log); 530/30 nm detector (FL1) = 500 V (log).

FC data were analyzed with Flowing Software 2.5.1 (Turku Centre for Biotechnology, Turku, Finland).

PMNs and monocytes were gated out based on their FSC–SSC characteristics; cell gates were defined in previous measurements with anti-CD11b-R-phycoerythrin antibodies (Dako, Glostrup, Denmark). Absolute change in geometric mean of FL1 (green) fluorescent intensity (ΔMFI) of the indicated cell types was compared with the change measured in supernatant control samples after 45 min incubation.

The uptake was also confirmed by confocal microscopic images (Zeiss, Oberkochen, Germany; LSM710 confocal laser scanning microscope equipped with EC Plan-Neoflural, Zeiss 40×/1.30 Oil DIC objective). Excitation and emission wavelengths were 488 and 494–651 nm, resp. Similar to FC experiments, 50 µl of 5×10^6/ml PMN or 10^7/ml mononuclear cell suspension was added to 500 µl aEV, sEV, apoEV sample or the control supernatant and incubated on a cover slip at 37°C. Samples were analyzed at 0 and 45 min with ZEN software (Zeiss).

2.9 | Measurement of phagocytic activity of PMNs

PMNs (120 µl of 5×10^6/ml) were added to 480 µL aEV, lysed aEV, sEV, apoEV sample or HBSS at 37°C in a linear shaker (0.18 g) for 45 min. aEV, lysed aEV, and sEV samples were prepared from 1.92×10^7 cells, whereas apoEV samples were derived from 0.96×10^7 cells.

In order to determine the phagocytic capacity, 5 different concentrations of opsonized *USA300* bacteria were used (1×10^8, 3×10^8, 1×10^9, 3×10^9, and 1×10^{10}/ml). From each concentration, 10 µl was added to 100 µl of the pretreated PMN populations at 37°C in a digital heating/shaking drybath for 20 min. Phagocytosis was stopped by adding 1 ml of ice-cold PBS to each sample. Uptake of *USA300* bacteria was detected with FC with the following settings: flow rate was held under 1,000 events/s; FSC = E—1 (log); SSC = 320 V (log); 530/30 nm detector (FL1) = 480 V (log). PMNs were gated out based on their FSC–SSC appearance. Autofluorescence intensity was measured with a PMN sample without bacteria. Geometric mean of FL1 (green) fluorescent intensity of PMN and percentage of PMN above the autofluorescence threshold were measured.

Similarly, kinetics of the phagocytic process was investigated by coincubating 600 µl of the abovementioned pretreated PMN populations with 60 µl of 3×10^8/ml opsonized *USA300* bacteria at 37°C in a digital heating/shaking drybath (1.89 g) for 20 min. At 0, 5, 10, 15, and 20 min, 100 µl of each suspension was added to 1 ml of ice-cold PBS. FL1 fluorescence was measured instantaneously with FC.

2.10 | Determination of the migratory potential of PMNs

PMNs (120 µl of 5×10^6/ml) were added to 480 µl aEV, lysed aEV, sEV, apoEV sample or HBSS at 37°C in a linear shaker (0.18 g) for 45 min. aEV, lysed aEV, and sEV samples were prepared from 1.92×10^7 cells, whereas apoEV samples were derived from 0.96×10^7 cells. The pretreated PMN samples were placed in the wells of a 3 µm pore Corning, NY, USA transwell cell culture plate coated with 10% FBS. Every well contained 2×10^5 cells. As a chemoattractant, 100 nM N-formylmethionyl-leucyl-phenylalanine was used. After 1 h incubation at 37°C, the transwell plate was centrifuged (Eppendorf 5810 R swing-bucket plate rotor, 3,220 *g*, 3 min, 4°C). Transmigrated cells were counted using an acid phosphatase assay[37] in a plate reader (Labsystems iEMS Reader MF; Thermo Scientific).

2.11 | Measurement of reactive oxygen species production of PMNs

PMNs (200 µl of 5 × 10^6/ml) were added to 2,000 µl aEV, lysed aEV, sEV, apoEV sample or HBSS at 37°C in a linear shaker (0.18 g) for 45 min. aEV, lysed aEV, and sEV samples were prepared from 4 × 10^7 cells, whereas apoEV samples were derived from 2 × 10^7 cells.

Lucigenin (5 mg/ml N,N′-dimethyl-9,9′-biacridinium dinitrate dissolved in DMSO, both from Sigma) was added in 1:100 volume ratio to the pretreated cells. White flat-bottom 96-well plates were coated with 10% FBS at room temperature for 1 h. Three parallel 180 µl samples of pretreated PMNs were activated in the coated wells with 20 µl 1 µM PMA. Changes in the luminescence were recorded for 90 min at 37°C with gentle shaking in a Varioskan multimode microplate reader (Thermo Fisher Scientific) every minute.

2.12 | Quantification of IL-8 secretion of PMNs

PMNs (120 µl of 2.5 × 10^7/ml) were added to 480 µl aEV, lysed aEV, sEV, apoEV sample or HBSS at 37°C in a linear shaker (0.18 g) for 3 h. aEV, lysed aEV, and sEV samples were prepared from 1.92 × 10^7 cells, whereas apoEV samples were derived from 0.96 × 10^7 cells.

Cells were centrifuged (500 *g*, 10 min, 4°C) and supernatants were analyzed for IL-8 with a human CXCL8/IL-8 DuoSet sandwich ELISA kit according to the manufacturer's instructions (R&D Systems)[38] in a plate reader (Labsystems iEMS Reader MF; Thermo Scientific, Minneapolis, MN, USA).

2.13 | Effect of EVs on coagulation

Turbidimetry was performed to study the EVs prothrombotic properties by registering the absorbance of samples at 340 nm at 37°C with a CLARIOStar microplate reader (BMG LABTECH, Ortenberg, Germany) as described previously.[39-41]

For clotting assays, aEV, lysed aEV, and sEV samples were prepared from 6.5 × 10^7 cells, whereas apoEV samples were derived from 2 × 10^7 cells.

To compare the positive effect of the aforementioned different types of EVs on the initiation of clotting in plasma, the change of absorbance was followed in microtiter plates. EVs were added to recalcified citrated human pooled plasma to reach a total volume of 104 µl with 12.5 mM calcium.

Furthermore, to assess the effects of EVs on the dynamics of clotting, the above described mixture was supplemented with 5 µl 100× diluted recombinant thromboplastin (TP) Dia-PT R (Diagon Kft, Budapest, Hungary) and the clotting curves were analyzed. A self-designed script running under the Matlab software (The Mathworks, Natick, MA, USA) was used to determine the maximum absorbance, and times to reach 10/50/90% of maximum absorbance.

2.14 | Preparation and culture of HUVECs

Cells were harvested from fresh umbilical cords obtained during normal delivery of healthy neonates (according to Helsinki Protocol, Semmelweis University Institutional Review Board specifically approved this study, (permission number: SETUKEB 141/2015), and

all participants provided their written informed consent to participate in this study), by collagenase digestion as described earlier.[42,43] HUVECs were kept in gelatin-precoated flasks in MCDB131 medium (Life Technologies, Carlsbad, CA, USA) completed with 5% heat-inactivated FCS, 2 ng/ml human recombinant epidermal growth factor (R&D Systems), 1 ng/ml human recombinant basic fibroblast growth factor (Sigma), 0.3% Insulin transferrin selenium (Life Technologies), 1% chemically defined lipid concentrate (Life Technologies), 1% glutamax (Life Technologies), 1% penicillin–streptomycin antibiotics (Sigma), 5 μg/ml ascorbic acid (Sigma), 250 nM hydrocortisone (Sigma), 10 mM HEPES (Sigma), and 7.5 U/ml heparin hereinafter referred to as Comp-MCDB131. Each experiment was performed on at least 3 independent primary HUVEC cultures from different individuals.

2.15 | Measurement of cytokine production of HUVECs by sandwich ELISA

Confluent layers (10^4 cell/well) of HUVECs were cultured in 96-well plates for 24 h in 100 μl Comp-MCDB131 medium supplemented with 20 μl EV sample. aEV, lysed aEV, and sEV samples were prepared from 5×10^6 cells, whereas apoEV samples were derived from 3.33×10^6 cells. IL-8 was measured in a plate reader (Infinite M1000 PRO; Tecan Group Ltd., Männedorf, Switzerland) by CXCL8/IL-8 DuoSet sandwich ELISA kit according to the manufacturer's protocol (R&D Systems) as described previously.[42,43]

2.16 | Detection of adhesion molecules by cellular ELISA

HUVECs were cultured in 96-well plates at confluent concentration in 100 μl Comp-MCDB131 medium for 1 day, then treated with different EV populations in 100 μl Comp-MCDB131 supplemented with 20 μl EV sample. aEV, lysed aEV, and sEV samples were prepared from 5×10^6 cells, whereas apoEV samples were derived from 3.33×10^6 cells. Previous studies have shown[42] that maximum expression of E-selectin and VCAM-1 were at 6 and 24 h, respectively, thus we detected the expression of adhesion molecules at these time points. Supernatants were removed for cytokine ELISA, cells were fixed in 1:1 methanol and acetone mixture and incubated with mouse-anti-human E-selectin or mouse-anti-human VCAM-1 (both from Bender MedSystems, GmbH, Vienna, Austria) for 1 h. Cells were washed with PBS-Tween containing 1% BSA then incubated with HRP-labeled goat-anti-mouse IgG (SouthernBiotech, Birmingham, AL, USA) for 1 h. Color reaction was developed by 3,3′,5,5′-tetramethylbenzidine (Thermo Fisher Scientific) and detected in a plate reader (Infinite M1000 PRO; Tecan Group Ltd.).

2.17 | Proteomic analysis of PMN-derived EVs

Proteomic analysis was performed as previously described.[32] Briefly, samples (45 μg) were lysed using 2% SDS at 65°C for 30 min, reduced, alkylated, and digested using trypsin (Promega, Madison, WI, USA).[44] Peptides were isolated through a YM-10 filter, desalted, and concentrated using NEST Group C18 PROTOTM UltraMicroSpin columns. Desalted samples were separated offline into 7 strong cation exchange (SCX) fractions using SCX MicroTrapTM (Michrom-Bruker, Auburn, CA, USA) prior to analysis by 1D-RP (C18) nanoflow UHPLC and nanoelectrospray-MS[45] on the Thermo LTQ-Orbitrap ELITE MS platform.

Data were acquired using Oribtrap ELITE in ETD decision tree method. All MS1 was acquired with the FTMS and MS2 acquired with the ITMS. All MS data were searched using PD1.4 with Sequest and Mascot (v2.4) in a decoy database search strategy against UniprotKB.

Search data result files were imported into Scaffold (v4.3.4 Proteome Software Inc., Portland, OR, USA) to control for <1.0% FDR with Peptide and Protein Prophet. Peptide and protein identifications were accepted if they could be established at greater than 95.0% probability by the Peptide Prophet[46] or the Protein Prophet[47] algorithm, respectively. Comparison of protein abundance among the EV groups was determined in Scaffold as the exponentially modified Protein Abundance Index (emPAI), as described by Ishihama et al.[48]

Proteomic data were analyzed further by the FunRich (version 3.1.3.) program to compare EV samples to each other or to the current FunRich (heatmap and integrin interactome) and UniProt human database (functional analysis).[49,50]

2.18 | Statistics

Plasma clotting results without TP were analyzed by Fisher's exact test; all other comparisons between 2 groups were analyzed by 2-tailed Student's *t*-tests or ANOVA. Exact statistical tests are indicated in the figure legends. All bar graphs show mean and +SEM. Difference was taken significant if P value was <0.05. * represents $P < 0.05$; ** represents $P < 0.01$; *** represents $P < 0.001$. Statistical analysis was performed using GraphPad Prism 8 for Windows (La Jolla, CA, USA).

In every experiment, "*n*" indicates the number of independent experiments from different donors, unless stated otherwise in the figure legend (Fig. 5).

Biologic variance between individual donors was considerable and also showed seasonal variations. Therefore, in addition to the summarized data, we present the normalized and paired values of individual experiments as well.

3 | RESULTS

3.1 | Characterization of PMN-derived EVs

First, we characterized the basic physical properties of the 3 types of PMN-derived EVs: those produced upon stimulation with opsonized zymosan (aEV) or spontaneously from fresh (sEV) or apoptotic cells (apoEV). The size distribution of the EV preparations was investigated by DLS (Fig. 1A). A broad peak was detected around 200 nm that disappeared upon treatment with Triton X-100 supporting the vesicular nature of the preparation. No significant differences were found among the 3 types of EVs. NTA was performed to quantitate both the number and the size of the EV populations. As shown in Fig. 1B, there were about twice as many particles in the aEV than in the sEV preparation. This difference corresponds to our earlier data obtained with flow cytometry.[12] There was no difference in the median diameter of sEV and aEV, whereas apoEV proved to be slightly larger (Fig. 1C). Electron microscopic images support that all 3 EV preparations contained membrane surrounded vesicles corresponding to "medium-size" EVs (Figs. 1D-1F).

Next, we show the major functional difference between the 3 types of PMN-derived EVs: only aEVs are able to impair bacterial growth (hence the name of antibacterial EVs), whereas sEV and apoEV lack this property (Fig. 1G).

In order to test the effect of the different EV types on neutrophil functions under stable conditions, we followed the fate of fluorescently labeled EVs upon encounter with PMN by flow cytometry. Monocytes served as a positive control. Figure S1A presents the original data in form of dot plots on the fluorescence distribution at the beginning and at the end of the 45 min incubation time in a representative experiment. Summarized data of the increase of mean fluorescent intensity (ΔMFI) are provided in Fig. S1B. At 45 min, a measurable increase of MFI occurred with all 3 EV populations in both cell types indicating that all 3 types of EVs get associated with PMNs. With confocal microscopic imaging we could verify that EVs are engulfed in PMN, as opposed to staying only attached on the surface of the cells (Fig. S1C).

In all the following experiments, cells were pretreated with EVs for 45 min, thus allowing sufficient time for uptake of vesicles.

3.2 | Effect of PMN-derived EVs on resting and activated PMNs

We measured the effect of PMN-derived EVs on reactive oxygen species (ROS) production. EVs isolated as described in Methods section, do not produce any detectable amount of ROS on their own.[12,32] None of the 3 different types of PMN-derived EVs have any significant effect on the basal superoxide production of resting neutrophils (Figs. 2A and 2E). Next, we tested whether EVs had any influence on stimulated ROS production. We applied as stimulator the pharmacologic agent PMA. PMA-induced superoxide production starts after a typical lag phase of variable length. We chose as characteristic parameters ROS production in the early phase at 10 min and at the maximum that occurred between 30 to 40 min. Opsonized zymosan is an inherent component of the aEV preparation and it may have various effects on PMN on its own. To assess the true effect of EVs, in these experiments, control PMNs were treated with the lysed fraction of the aEV preparation (details see in Methods). Figure 2 shows both the summarized data of the absolute values (Figs. 2A and 2E) and the paired data related to the relevant control from each experiment (Figs. 2B-2D and 2F-2H). After 10 min in the presence of sEV or apoEV, ROS production was significantly diminished (Figs. 2A, 2C-2D). In contrast, in the presence of aEVs, there was a significant and consistent increase of ROS production as compared to the control (Figs. 2A and 2B). Maximal ROS production was also significantly and consistently higher than the control in the presence of aEV and lower in the presence of sEV (Figs. 2E-2G). The difference in the presence of apoEV was not significant (Figs. 2E and 2H). We thus observed opposing effect of aEV and sEV upon stimulated ROS production. A third type of effect was observed with apoEVs: by reducing the early but not affecting the maximal ROS production they induced a right-shift of the time curve.

Alteration of cytokine secretion upon EV treatment was investigated previously in monocytes,[17-21,25] but not in PMN. Therefore, we tested cytokine secretion from neutrophils after encountering the different EV populations. Resting PMNs produce low amount of IL-8, which was dramatically increased by opsonized zymosan, which served as positive control

(Fig. 3A). Even the zymosan remnants present in the aEV preparation were able to increase IL-8 secretion approximately fourfold (lysed aEV column in Fig. 3A). In order to test exclusively the effect of the different EV preparations, all the samples contained the same amount of lysed aEV. As summarized in Fig. 3A, IL-8 release was significantly increased by aEV, but decreased by sEV. These changes were consistently observed in all experiments (Figs. 3B and 3C). In contrast, IL-8 release in the presence of apoEV showed no significant change (Fig. 3D).

In the following experiments, we compared phagocytosis, another basic neutrophil function, in the absence or following pretreatment by different types of PMN-derived EVs. In Fig. S2, we show both the kinetics of uptake of fluorescent *S. aureus* (panels A, C, and E) and the maximal uptake in case of different ratios of bacteria to PMNs (panels B, D, and F). None of the EVs had any significant effect on the engulfment of fully opsonized bacteria.

Finally, we tested the effect of EVs on neutrophil migration in a chemotactic gradient (Fig. S3). Again, none of the EVs had significant or consistent effect.

Taken together, our results show that aEV and sEV have opposite effects on ROS production and cytokine secretion, whereas apoEV only delayed ROS production. Phagocytosis and chemotactic migration were not influenced by any of the EVs.

3.3 | Effect of PMN-derived EVs on endothelial cells

The first reports on biologic effects of PMN-derived EVs showed an increase of proinflammatory cytokine secretion from endothelial cells.[28,29] In view of the observed opposing effect of sEV and aEV on IL-8 secretion from neutrophils, we tested their effect also on HUVECs. In this setting, only aEV stimulated a significant and reproducible increase of IL-8 secretion (Figs. 4A and 4D), whereas sEV and apoEV had no consistent effect (Figs. S3A and D).

To gain further insight in dissimilar effectivity of neutrophil-derived EVs, we tested 2 activation markers on the endothelial cells: E-selectin and VCAM-1. The expression of both surface markers was significantly and reproducibly increased by aEVs (Figs. 4B, 4C, 4E, and 4F). In contrast, neither sEV nor apoEV had any consistent effect (Fig. S3).

Our data obtained on endothelial cells further support the diverging effect of EVs generated by resting (sEV) or activated (aEV) neutrophils.

3.4 | Effect of PMN-derived EVs on coagulation

Increased blood clotting was reported as a common property of EVs released from different cell types.[2] Based on our above results, we asked whether all EV types have similar capacity in enhancing coagulation.

We tested the system in 2 different settings. First, we explored the procoagulant activity of the EVs themselves (in the absence of added TP). In the experiments presented in Figs. 5A-5F, we detected the frequency of coagulation in the presence of the different types of EVs. Panels A–C provide the exact numbers of cases where coagulation did or did not occur,

which allowed the statistical analysis of data, whereas panels D–F present the ratio of events where coagulation did happen. For aEVs, the frequency of coagulation was almost the same in case of intact or lysed aEVs, suggesting that coagulation was initiated by some other component (e.g., opsonized zymosan remnant) but not the EVs themselves. In cases of both sEV and apoEV, the frequency of coagulation was significantly higher in the presence of EVs than in their absence. ApoEV proved to be the most effective, initiating coagulation in over one-third of the measurements.

In the second test, coagulation time was measured in a system initiated by TP. As shown in Figs. 5G-5I, the presence of apoEV reduced coagulation time significantly and consistently. The presence of sEV resulted in a decreasing tendency but the effect was not statistically significant. Similar to the previous test, the effect of aEV was weak.

Our results on coagulation support the functional diversity of the different types of PMN-derived EVs, with apoEV having the largest and aEV the smallest effect.

3.5 | Proteomic analysis of PMN-derived EVs

We carried out proteomic analysis of the 3 distinct EV preparations in order to relate protein composition to the observed functional divergences. A total of 774 proteins could be identified in the 3 EV populations. The variety of proteins in aEVs is less than the half of that in the other 2 EV types (284 vs. 636 and 705, respectively) and the number of unique proteins is also remarkably lower (Fig. 6A). The differences in the abundance of individual proteins compared with the average of the 3 EV types is shown in the heat map of Fig. 6B. A large cluster of proteins is significantly underrepresented and another cluster significantly overrepresented in aEVs compared with either sEV or apoEV; however, the latter 2 samples also showed characteristic differences. Next, the abundance of specific groups of proteins was analyzed (Fig. 6C). The origin of proteins shows that aEVs contain more proteins of plasma membrane and less proteins of nucleoplasmic origin than either sEV or apoEV, and they are also enriched in components of focal adhesions and exosomes. Categorizing proteins according to biologic function shows that aEVs contain more proteins involved in cell adhesion and immune response than the other 2 EV types, whereas proteins associated to the MAPK cascade are less abundant. As for molecular functions, several types of binding proteins, including integrin binding proteins are enriched in aEVs.

Recently, we have identified Mac1 integrin as the critical surface receptor that initiates formation of aEVs.[36] Previously we showed a potential role of Mac1 in the aggregation of bacteria and aEVs related to impaired bacterial killing.[12] Therefore, we analyzed in detail the interactome of integrins identified in the distinct EV preparations. As indicated by the proportion of red dots in Fig. 6D, aEVs contain a higher proportion of proteins interacting with integrins.

4 | DISCUSSION

Using PMN as model cell type, we show in this study that EVs generated under different physiologically or pathologically relevant conditions from the same cell exert divergent and selective effects on cells and functions in their environment (Table 1). In previous

studies, we demonstrated the difference between aEV and sEV in their action on bacterial growth and in their protein composition.[12,32] This line of observations is now extended by demonstrating their opposing effect on ROS production and IL-8 secretion from PMN, and their distinct effects on endothelial cells. Importantly, we also show differences in their influence on coagulation.

Interestingly, we observed some differences between the effects of sEV and apoEV as well. The latter type did not decrease maximal ROS production and IL-8 release from neutrophils, but had a strong and clear procoagulant effect. Production of sEV seems to be a constitutive property of neutrophils. In our hands, no inhibitor or genetic deficiency of receptors or signaling molecules had any influence on sEV generation.[36,51] Neutrophils being short-lived cells that go in spontaneous apoptosis, it could be envisaged that sEV are produced by a few cells going into apoptosis during the short (20 min) incubation time before we collect the vesicles. However, the observed differences in the actions and the protein composition between sEV and apoEV indicate separate EV populations.

In the current study, we compare 3 types of EVs, which are present under different conditions in circulating blood.[12] sEV and apoEV are produced from resting, not specifically stimulated cells. They have no effect or mitigate neutrophil and endothelial cell activation. These findings are consistent with numerous previous reports on anti-inflammatory effects of PMN-derived EVs on monocytes and macrophages.[14,20,23,52] In contrast, aEVs are produced upon stimulation by opsonized particles, typical under infectious conditions.[12] Our present data indicate that aEVs activate select proinflammatory functions in both neutrophils and endothelial cells. These observations are consistent with data on proinflammatory properties of PMN-derived EVs.[15,17,18,24,25,28,29]

Finally, it is important to note that neither phagocytosis nor chemotactic migration was affected by any of the EVs, supporting the selective nature of EV actions.

Many previous studies have concluded that EVs are able both to stimulate and to dampen immune functions.[3,53,54] However, those studies summarized the effects of EVs issued from very different sources and actions on most different players of the complicated immune reaction. The novelty of our study resides in demonstrating that the same cells are able to transmit either anti-inflammatory or proinflammatory signals via EVs, depending on the environmental cues.

The divergent effects communicated by the different types of EVs are unlikely to be caused by one common mechanism. The time scale of the demonstrated effects alone suggests different mechanisms. Coagulation occurs in a few minutes, hence differences in the surface components can be envisaged as the decisive factors. Alteration of ROS production was evident in 10–30 min, suggesting posttranslational modification rather than alteration of gene expression as potential mechanism. Cytokine secretion from PMNs and HUVEC as well as appearance of HUVEC surface markers occurred after several hours, suggesting an alteration in gene expression. The observed differences in protein composition (Fig. 6A), abundance (Fig. 6B), and pattern (Figs. 6C and 6D) among the 3 types of EVs can account for both shortterm and long-term functional alterations. The specific signaling pathways

involved in the diverging or opposing effects revealed in this study have to be deciphered in future investigations.

Production of EVs with diverse and selective effect is probably not the unique property of PMNs. Numerous studies demonstrated differences in the composition of EVs secreted from the same cell under different conditions. In contrast, functional differences were tested only by a few publications.[18,31] In the present study, we revealed that EV effects can be divergent and even antagonistic depending on the environmental conditions prevailing at time of EV biogenesis. At the dawn of therapeutic usage of EVs and EV-related preparations, we call the attention to the need of detailed comparative examination of functional properties of EVs.

Supplementary Material

Refer to Web version on PubMed Central for supplementary material.

ACKNOWLEDGMENTS

The authors would like to thank to Professor Kraszimir Kolev, Drs. László Cervenák and Ádám Farkas for helpful and constructive discussions and Regina Tóth-Kun for expert and devoted technical assistance. Experimental work was supported by research grant No. 119236 from NKFIH and 2.3.2.-16 from VEKOP to E.L., and by the Higher Education Institutional Excellence Programme of the Ministry of Human Capacities in Hungary, within the framework of the molecular biology thematic program of Semmelweis University. This paper was supported by the János Bolyai Research Scholarship of the Hungarian Academy of Sciences.

Abbreviations:

aEV	antibacterial EV
apoEV	apoptotic EV
DLS	dynamic light scattering
EV	extracellular vesicle
FC	flow cytometry
FSC	forward scatter
MFI	mean fluorescent intensity
NTA	nanoparticle tracking analysis
PMN	polymorphonuclear cell (here: neutrophilic granulocyte)
ROS	reactive oxygen species
sEV	spontaneous EV
SSC	side scatter
TP	thromboplastin

REFERENCES

1. Raposo G, Stoorvogel W. Extracellular vesicles: exosomes, microvesicles, and friends. J Cel Biol. 2013;200:373–383.
2. Yáñez-Mó M, Siljander PRM, Andreu Z, et al. Biological properties of extracellular vesicles and their physiological functions. J Extracell Vesicles. 2015;4:27066. [PubMed: 25979354]
3. El Andaloussi S, Mäger I, Breakefield XO, et al. Extracellular vesicles: biology and emerging therapeutic opportunities. Nat Rev Drug Discov. 2013;12:347–357. [PubMed: 23584393]
4. Allan DS, Tieu A, Lalu M, et al. Concise review: mesenchymal stromal cell-derived extracellular vesicles for regenerative therapy and immune modulation: progress and challenges toward clinical application. Stem Cells Transl Med. 2019:1–7.
5. Mendt M, Rezvani K, Shpall E. Mesenchymal stem cell-derived exosomes for clinical use. Bone Marrow Transplant. 2019;54:789–792. [PubMed: 31431712]
6. Tarasov VV, Svistunov AA, Chubarev VN, et al. Extracellular vesicles in cancer nanomedicine. Semin Cancer Biol. 2019:0–1.
7. Marzano M, Bejoy J, Cheerathodi MR, et al. Differential effects of extracellular vesicles of lineage-specific human pluripotent stem cells on the cellular behaviors of isogenic cortical spheroids. Cells. 2019;8:993.
8. Chance TC, Rathbone CR, Kamucheka RM, et al. The effects of cell type and culture condition on the procoagulant activity of human mesenchymal stromal cell-derived extracellular vesicles. J Trauma Acute Care Surg. 2019;87:S74–S82. [PubMed: 31246910]
9. Tucher C, Bode K, Schiller P, et al. Extracellular vesicle subtypes released from activated or apoptotic T-lymphocytes carry a specific and stimulus-dependent protein cargo. Front Immunol. 2018;9:534. [PubMed: 29599781]
10. Chen Q, Takada R, Noda C, et al. Different populations of Wnt-containing vesicles are individually released from polarized epithelial cells.Sci Rep. 2016;6:35562. [PubMed: 27765945]
11. Nieuwland R, Berckmans RJ, McGregor S, et al. Cellular origin and procoagulant properties of microparticles in meningococcal sepsis. Blood. 2000;95:930–935. [PubMed: 10648405]
12. Timár CI, Lorincz ÁM, Csépányi-Kömi R, et al. Antibacterial effect of microvesicles released from human neutrophilic granulocytes. Blood. 2013;121:510–518. [PubMed: 23144171]
13. Dalli J, Norling LV, Montero-Melendez T, et al. Microparticle alpha-2-macroglobulin enhances pro-resolving responses and promotes survival in sepsis. EMBO Mol Med. 2014;6:27–42. [PubMed: 24357647]
14. Dalli J, Norling LV, Renshaw D, et al. Annexin 1 mediates the rapid anti-inflammatory effects of neutrophil-derived microparticles. Blood. 2008;112:2512–2519. [PubMed: 18594025]
15. Majumdar R, Tavakoli Tameh A, Parent CA. Exosomes mediate LTB4 release during neutrophil chemotaxis. PLoS Biol. 2016;14:e1002336. [PubMed: 26741884]
16. Salei N, Hellberg L, Köhl J, et al. Enhanced survival of Leishmania major in neutrophil granulocytes in the presence of apoptotic cells. PLoS One. 2017;12:1–15.
17. Byrne A, Reen DJ. Lipopolysaccharide induces rapid production of IL-10 by monocytes in the presence of apoptotic neutrophils. J Immunol. 2002;168:1968–1977. [PubMed: 11823533]
18. Alvarez-Jiménez VD, Leyva-Paredes K, García-Martínez M, et al. Extracellular vesicles released from Mycobacterium tuberculosis-infected neutrophils promote macrophage autophagy and decrease intracellular mycobacterial survival. Front Immunol. 2018;9:272. [PubMed: 29520273]
19. Ren Y, Xie Y, Jiang G, et al. Apoptotic cells protect mice against lipopolysaccharide-induced shock. J Immunol. 2008;180:4978–4985. [PubMed: 18354223]
20. Gasser O, Schifferli JA. Activated polymorphonuclear neutrophils disseminate anti-inflammatory microparticles by ectocytosis. Blood. 2004;104:2543–2548. [PubMed: 15213101]
21. Eken C, Martin PJ, Sadallah S, et al. Ectosomes released by polymorphonuclear neutrophils induce a MerTK-dependent anti-inflammatory pathway in macrophages. J Biol Chem. 2010;285:39914–39921. [PubMed: 20959443]

22. Ren Y, Stuart L, Lindberg FP, et al. Nonphlogistic clearance of late apoptotic neutrophils by macrophages: efficient phagocytosis independent of β2 integrins. J Immunol. 2001;166:4743–4750. [PubMed: 11254736]
23. Duarte TA, Noronha-Dutra AA, Nery JS, et al. Mycobacterium tuberculosis-induced neutrophil ectosomes decrease macrophage activation. Tuberculosis. 2012;92:218–225. [PubMed: 22391089]
24. Dalli J, Montero-Melendez T, Norling LV, et al. Heterogeneity in neutrophil microparticles reveals distinct proteome and functional properties. Mol Cell Proteomics. 2013;12:2205–2219. [PubMed: 23660474]
25. Johnson BL, Midura EF, Prakash PS,et al. Neutrophil derived microparticles increase mortality and the counter-inflammatory response in a murine model of sepsis. Biochim Biophys Acta Mol Basis Dis. 2017;1863:2554–2563. [PubMed: 28108420]
26. Eken C, Gasser O, Zenhaeusern G, et al. Polymorphonuclear neutrophil-derived ectosomes interfere with the maturation of monocyte-derived dendritic cells. J Immunol. 2008;180:817–824. [PubMed: 18178820]
27. Shen G, Krienke S, Schiller P, et al. Microvesicles released by apoptotic human neutrophils suppress proliferation and IL-2/IL-2 receptor expression of resting T helper cells. Eur J Immunol. 2017;47:900–910. [PubMed: 28295230]
28. Mesri M, Altieri DC. Leukocyte microparticles stimulate endothelial cell cytokine release and tissue factor induction in a JNK1 signaling pathway. J Biol Chem. 1999;274:23111–23118. [PubMed: 10438480]
29. Mesri M, Altieri DC. Endothelial cell activation by leukocyte microparticles. J Immunol. 1998;161:4382–4387. [PubMed: 9780216]
30. Oehmcke S, Westman J, Malmström J, et al. A novel role for procoagulant microvesicles in the early host defense against Streptococcus pyogenes. PLoS Pathog. 2013;9:e1003529. [PubMed: 23935504]
31. Martin KR, Kantari-Mimoun C, Yin M, et al. Proteinase 3 is a phosphatidylserine-binding protein that affects the production and function of microvesicles. J Biol Chem. 2016;291:10476–10489. [PubMed: 26961880]
32. Lorincz AM, Schutte M, Timar CI, et al. Functionally and morphologically distinct populations of extracellular vesicles produced by human neutrophilic granulocytes. J Leukoc Biol. 2015;98:583–589. [PubMed: 25986013]
33. Lőrincz ÁM, Szeifert V, Bartos B, et al. New flow cytometry-based method for the assessment of the antibacterial effect of immune cells and subcellular particles. J Leukoc Biol. 2018;103:955–963. [PubMed: 29513908]
34. Lőrincz ÁM, Timár CI, Marosvári KA, et al. Effect of storage on physical and functional properties of extracellular vesicles derived from neutrophilic granulocytes. J Extracell Vesicles. 2014;3:25465. [PubMed: 25536933]
35. Rada BK, Geiszt M, Káldi K, et al. Dual role of phagocytic NADPH oxidase in bacterial killing. Blood. 2004;104:2947–2953. [PubMed: 15251984]
36. Lőrincz ÁM, Bartos B,Szombath D, et al. Role of Mac-1 integrin in generation of extracellular vesicles with antibacterial capacity from neutrophilic granulocytes. J Extracell Vesicles. 2020;9:1698889. [PubMed: 31853340]
37. Lowell CA, Fumagalli L, Berton G. Deficiency of src family kinases p59/61hck and p58c-fgr results in defective adhesion-dependent neutrophil functions. J Cell Biol. 1996;133:895–910. [PubMed: 8666673]
38. Karmakar M, Katsnelson M, Malak HA, et al. Neutrophil IL-1β processing induced by pneumolysin is mediated by the NLRP3/ASC inflammasome and caspase-1 activation and is dependent on K + efflux. J Immunol. 2015;194:1763–1775. [PubMed: 25609842]
39. Varjú I, Farkas VJ, Kohidai L, et al. Functional cyclophilin D moderates platelet adhesion, but enhances the lytic resistance of fibrin. Sci Rep. 2018;8:1–13. [PubMed: 29311619]
40. Farkas ÁZ, Farkas VJ, Szabó L, et al. Structure, mechanical, and lytic stability of fibrin and plasma coagulum generated by Staphylocoagulase from Staphylococcus aureus. Front Immunol. 2019;10:2967. [PubMed: 31921206]

41. Longstaff C, Varjú I, Sótonyi P, et al. Mechanical stability and fibrinolytic resistance of clots containing fibrin, DNA, and histones. J Biol Chem. 2013;288:6946–6956. [PubMed: 23293023]
42. Makó V, Czúcz J, Weiszhár Z, et al. Proinflammatory activation pattern of human umbilical vein endothelial cells induced by IL-1β, TNF-α, and LPS. Cytom Part A. 2010;77:962–970.
43. Jani PK, Kajdácsi E, Megyeri M, et al. MASP-1 induces a unique cytokine pattern in endothelial cells: a novel link between complement system and neutrophil granulocytes. PLoS One. 2014;9:10–13.
44. Uriarte SM, Rane MJ, Merchant ML, et al. Inhibition of neutrophil exocytosis ameliorates acute lung injury in rats. Shock. 2013;39:286–292. [PubMed: 23364427]
45. Baba SP, Hoetker JD, Merchant M, et al. Role of aldose reductase in the metabolism and detoxification of carnosine-acrolein conjugates. J Biol Chem. 2013;288:28163–28179. [PubMed: 23928303]
46. Keller A, Nesvizhskii AI, Kolker E, et al. Empirical statistical model to estimate the accuracy of peptide identifications made by MS/MS and database search. Anal Chem. 2002;74:5383–5392. [PubMed: 12403597]
47. Uriarte SM, Powell DW, Luerman GC, et al. Comparison of proteins expressed on secretory vesicle membranes and plasma membranes of human neutrophils. J Immunol. 2008;180:5575–5581. [PubMed: 18390742]
48. Ishihama Y, Oda Y, Tabata T, et al. Exponentially modified protein abundance index (emPAI) for estimation of absolute protein amount in proteomics by the number of sequenced peptides per protein. Mol Cell Proteomics. 2005;4:1265–1272. [PubMed: 15958392]
49. Pathan M, Keerthikumar S, Ang C-S, et al. FunRich: an open access standalone functional enrichment and interaction network analysis tool. Proteomics. 2015;15:2597–2601. [PubMed: 25921073]
50. Pathan M, Keerthikumar S, Chisanga D, et al. A novel community driven software for functional enrichment analysis of extracellular vesicles data. J Extracell Vesicles. 2017;6:1321455. [PubMed: 28717418]
51. Lőrincz ÁM, Szeifert V, Bartos B, et al. Different calcium and src family kinase signaling in Mac-1 dependent phagocytosis and extracellular vesicle generation. Front Immunol. 2019;10:1–11. [PubMed: 30723466]
52. Rhys HI, Dell'Accio F, Pitzalis C, et al. Neutrophil microvesicles from healthy control and rheumatoid arthritis patients prevent the inflammatory activation of macrophages. EBioMedicine. 2018;29:60–69. [PubMed: 29449195]
53. Wiklander OPB, Brennan M, Lötvall J, et al. Advances in therapeutic applications of extracellular vesicles. Sci Transl Med. 2019;11:1–16.
54. Théry C, Ostrowski M, Segura E. Membrane vesicles as conveyors of immune responses. Nat Rev Immunol. 2009;9:581–593. [PubMed: 19498381]

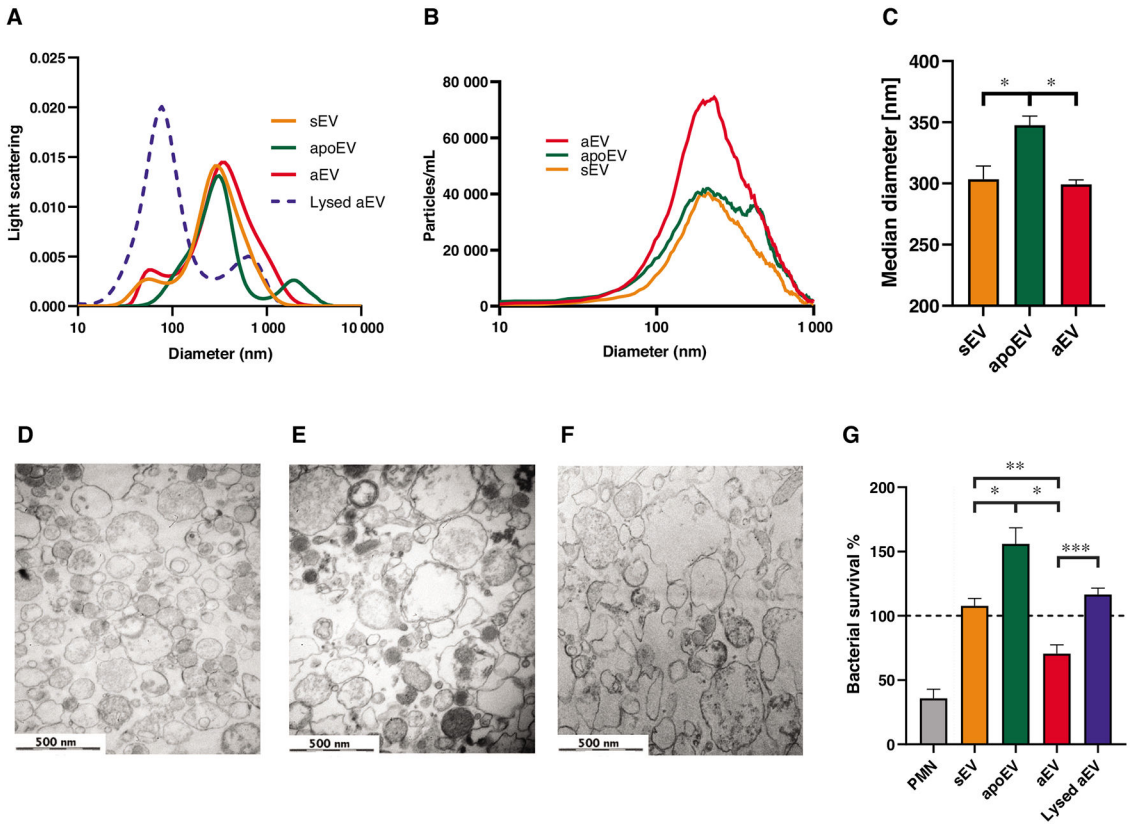

FIGURE 1. Characterization of EV samples.

(A) Size distribution spectra of EVs measured by DLS. Broken line represents 0.1% Triton X-100-treated aEV. Representative results out of 3 similar experiments. (**B**) Particle size distribution of EVs measured by NTA. ApoEV were measured in a 10-fold dilution in order to stay within optimal detection ranges. Representative results out of 3 similar experiments. (C) Particle median diameter of EVs measured by NTA. Data were compared by using RM 1-way ANOVA coupled with Sidak's post hoc test; $n = 3$. Error bars represent mean + SEM. (D–F) Representative electron microscopic images of sEV (D), aEV (E), and apoEV (F). Original magnification is 30,000×. Representative pictures out of 3 similar experiments. (G) Bacterial survival in the presence of different types of EVs released from 5×10^6 PMNs. Data were compared by using RM 1-way ANOVA coupled with Sidak's post hoc test; $n = 4$. Error bars represent mean + SEM. 100% represents the initial bacterial count

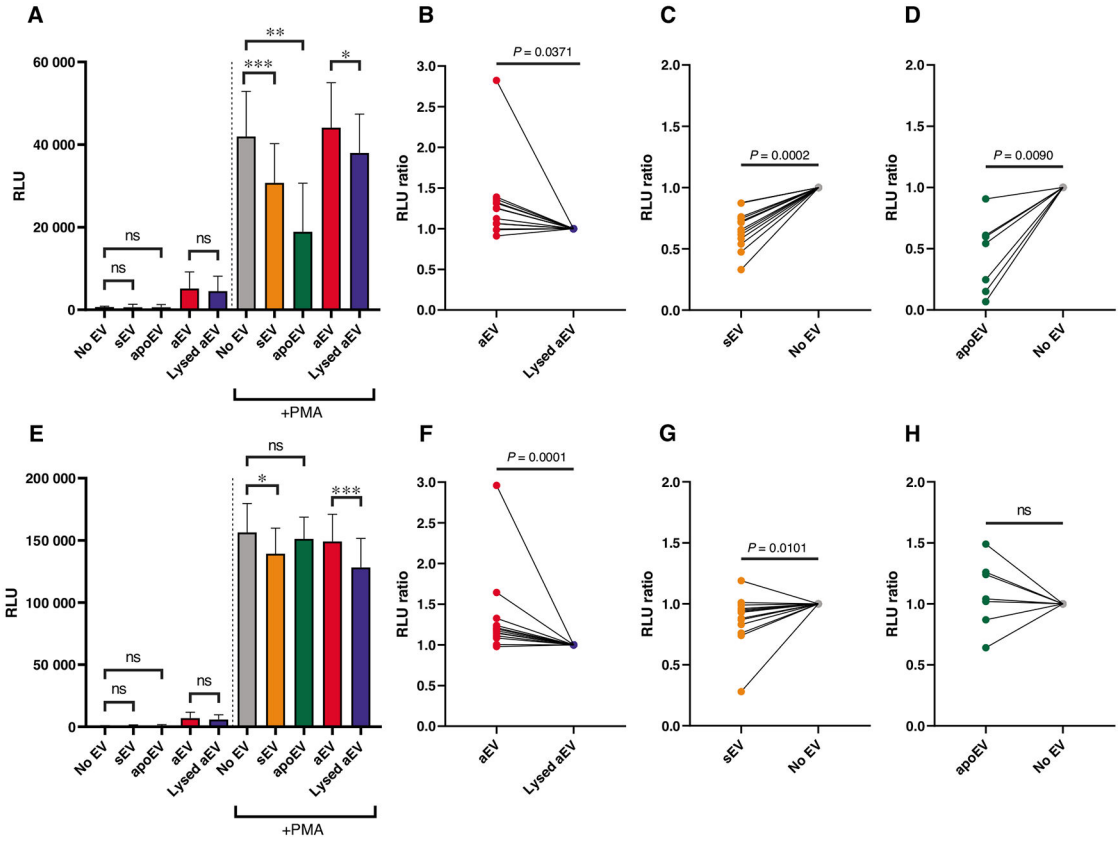

FIGURE 2. Effect of EVs on the ROS production of PMN.

PMNs were pretreated for 45 min with the indicated EV or control, then left unstimulated or activated with 100 nM PMA. ROS production was determined at 10 min after activation (A–D) and at the peak intensity of the curve, typically at 30 to 40 min (E–H). Panels (A) and (E) show the summarized ROS production of the EV-pretreated PMN, (B–D) and (F–H) show the normalized data pairs from each experiment. Data were normalized to their adequate controls ("aEV" to "Lysed aEV," "sEV" and "apoEV" to "No EV"). Raw data were compared using paired Student's *t*-test; $n = 13$ for aEV and sEV; $n = 7$ for apoEV. Error bars represent mean + SEM

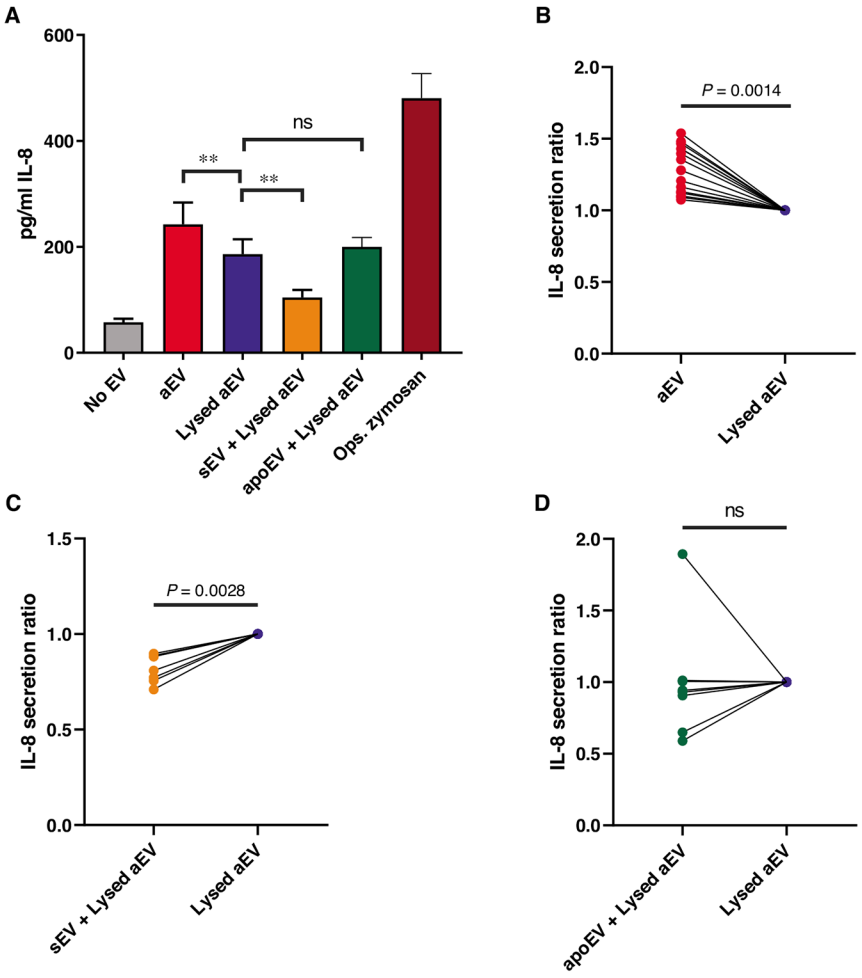

FIGURE 3. Effect of EVs on the IL-8 production of PMN.

PMNs were treated for 3 h with 1 of the 3 EV populations or their controls. IL-8 amount of the supernatant was quantified with ELISA. Panel (A) shows the summarized changes in IL-8 production of the EV-treated cells. Panels (B)–(D) show the normalized data pairs from each experiment. Data were normalized to their adequate controls ("aEV" to "Lysed aEV," "sEV" and "apoEV" to "No EV"). Raw data were compared using paired Student's *t*-test; $n = 15$ for aEV; $n = 7$ for sEV; $n = 8$ for apoEV. Error bars represent mean + SEM

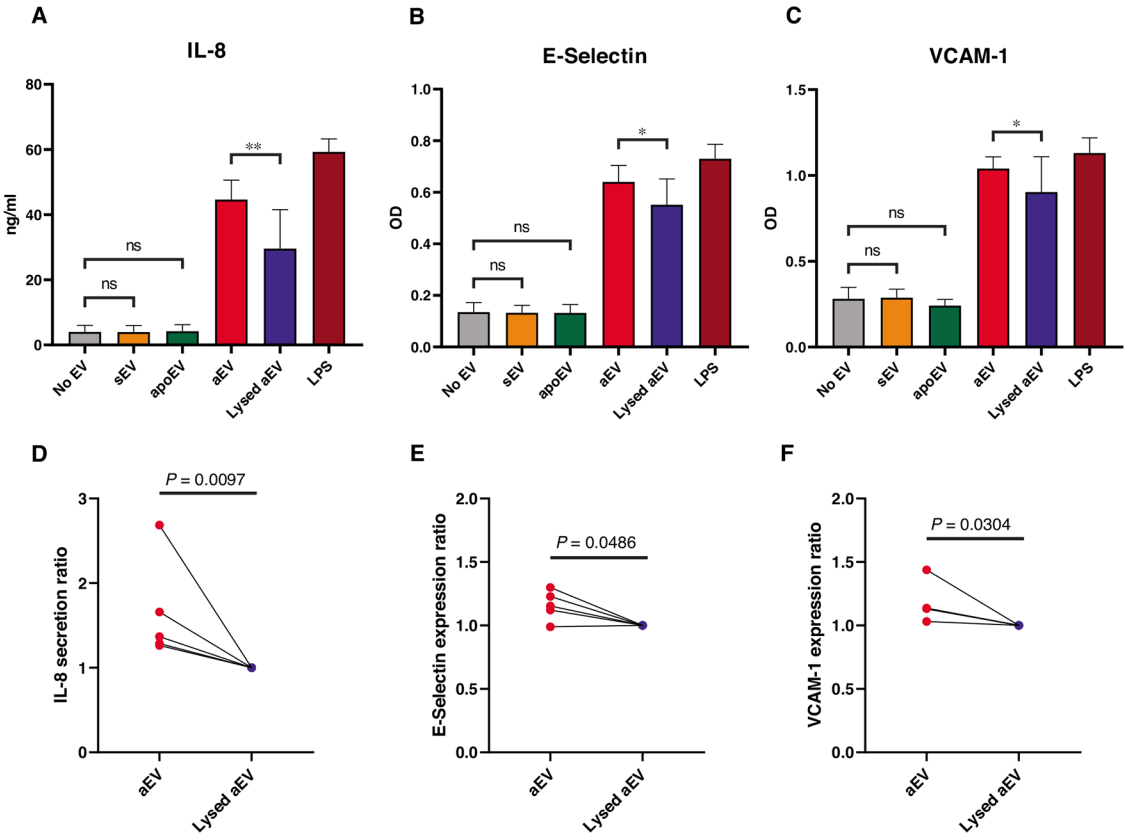

FIGURE 4. Effect of EVs on endothelial cells.

HUVEC were pretreated for 6 h (E-Selectin) or 24 h (VCAM-1 and IL-8) with 1 of the 3 EV populations or their controls. IL-8 amount of the supernatant was quantified with ELISA (A and D). E-Selectin and VCAM-1 expression was determined by cellular ELISA (B, C, E, and F). Panels (A)–(C) show the summarized changes in IL-8 secretion, E-Selectin, and VCAM-1 expression of the EV-treated cells. Panels (D)–(F) show the normalized data pairs for aEV or control-treated cells from each experiment. Data were normalized to their adequate controls ("aEV" to "Lysed aEV", "sEV" and "apoEV" to "No EV"). Raw data were compared using paired Student's *t*-test; $n = 5$. Error bars represent mean + SEM

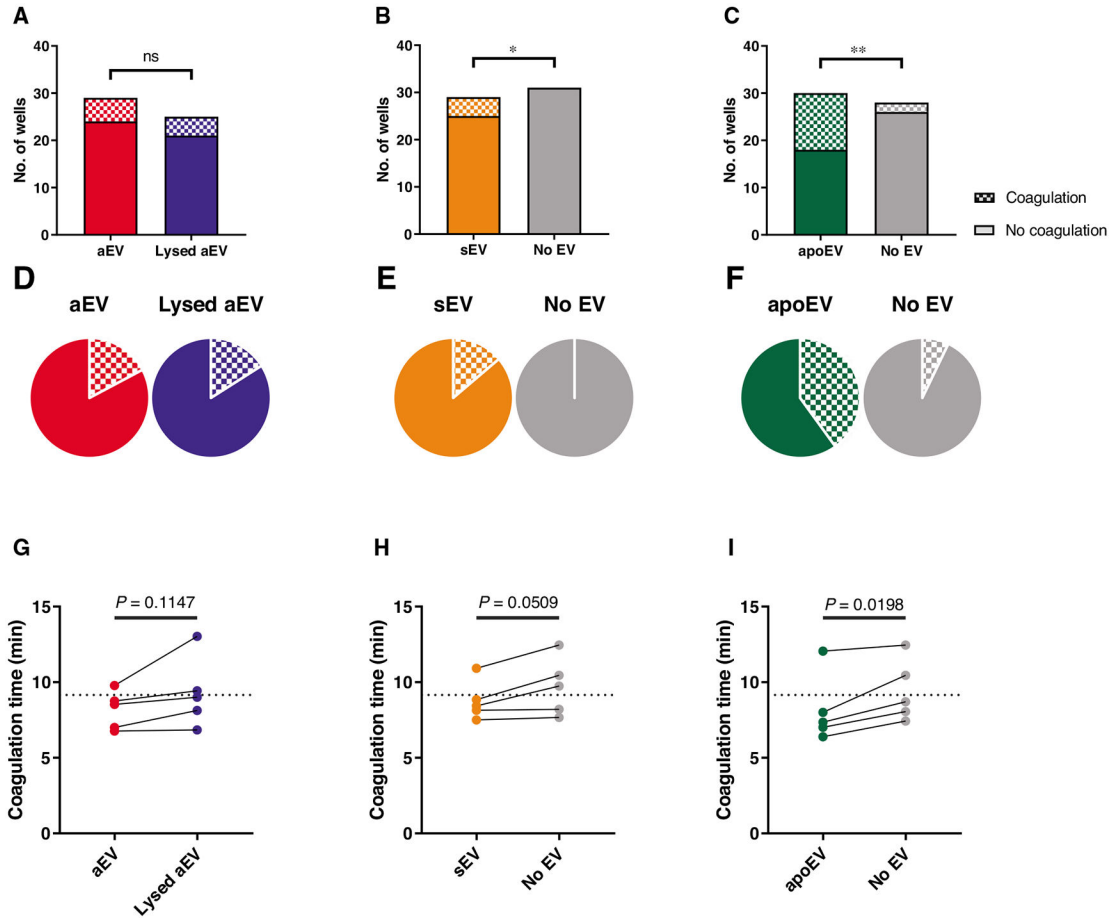

FIGURE 5. Effect of EVs on coagulation.

One of the 3 EV populations or their controls were mixed with pooled citrated human plasma in the absence (A–F) or presence (G–I) of thromboplastin followed by recalcification with Ca-HEPES. Panels (A)–(C) show the absolute numbers of coagulated and not coagulated wells in each sample. Panels (D)–(F) represent the percentage of coagulated wells based on the same data. Panels (G)–(I) show the time needed for 50% of the coagulation process in the thromboplastin-treated samples (raw data pairs). The dotted lines on (G)–(I) show the average coagulation time of the "No EV" samples. Data were compared using Fisher's exact test (A–F) and paired Student's *t*-test (G–I). $n = 29$ wells from 7 donors for aEV and sEV; $n = 30$ wells from 6 donors for apoEV (A–F). $n = 5$ from 5 donors (G–I)

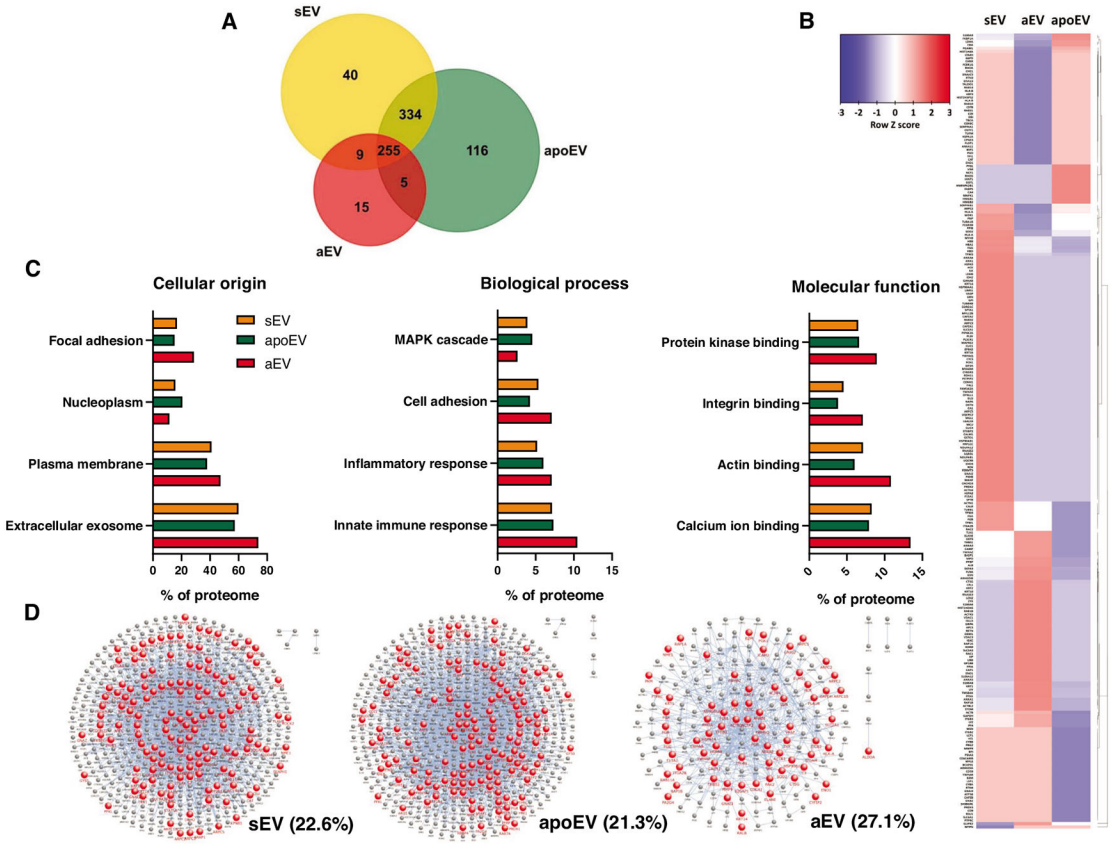

FIGURE 6. Proteomic analysis of EV populations.

(A) Comparison of protein presence in different EV populations using Venn diagram. Equal protein amount was analyzed (45 μg). The size of the set is proportional to the number of identified proteins. (B) Protein enrichment heat map of the 3 different EV populations normalized to each row. Proteins are clustered according to the calculated dendrogram by FunRich. (C) Analysis of protein content according to cellular origin, biologic process, and molecular function. (D) Integrin interactome of sEV, apoEV, and aEV. Red nodes represent proteins that are part of the integrin interactome. Blue nodes represent identified proteins that are not the part of the integrin interactome. Percentage of integrin interactome proteins to all proteins is indicated

TABLE 1

Summarized effects of PMN-derived EVs

	aEV	sEV	apoEV
Maximal ROS production	↑	↓	–
Early ROS production	↑	↓	↓
IL-8 production of PMN	↑	↓	–
IL-8 secretion of HUVEC	↑	–	–
E-selectin expression of HUVEC	↑	–	–
VCAM-1 expression of HUVEC	↑	–	–
Coagulation (no TP)	–	↑	↑
Coagulation time (TP)	–	–	↓
Phagocytosis	–	–	–
Migration	–	–	–

Arrows represent the observed statistically significant changes upon pretreatment with different EV populations compared to their adequate controls.